Tissue Specific Arterial Spin Labeling fMRI: A Superior Method for Imaging Cerebral Blood Flow in Aging and Disease

Yujie Qiu[1], Ajna Borogovac[2], Andrew Laine[3], Joy Hirsch[4], Iris Asllani[1*]

Abstract— **Cerebral blood flow (CBF) is a physiological correlate of brain function and metabolism and as such an essential parameter for investigating how aging and disease affect the brain. Arterial spin labeling (ASL) is an fMRI method that provides absolute measurement of CBF non-invasively and with higher spatial resolution than non-MRI methods. However, application of ASL in older populations is hampered by partial volume effects (PVE) and tissue dependent changes in CBF. We have developed a tissue-specific ASL method (ts-ASL) that provides 'flow density' measures by quantifying CBF for each tissue separately and independently of tissue content. Using simulated functional and structural images, we investigated the effects of brain atrophy and random noise on the SNR of GM CBF measured with conventional and ts-ASL. Results showed that: (1) For all noise levels, the SNR of ts-ASL was higher. For example, for a random Gaussian noise with standard deviation σ = 4, the SNR of GM CBF obtained with ts-ASL was ~3 times higher than the SNR of the conventional method. (2) In contrast to conventional ASL, which was substantially affected by brain atrophy, ts-ASL was virtually independent of it. (3) The sensitivity of ts-ASL for detecting focal changes in CBF (ΔCBF) in the presence of atrophy and noise was also higher compared to the conventional method. In hippocampus, for 15% atrophy and Gaussian noise with σ = 4, conventional and ts-ASL retrieved 73% and 90% of the modeled ΔCBF, respectively. Taken together, these results indicate that ts-ASL may be better suited for measuring CBF in the presence of atrophy and random noise, both of which are expected to increase with aging and disease.**

I. Introduction

Functional MRI methods rely on fast image acquisition techniques such as echo-planar imaging (EPI) to achieve the temporal resolution needed for detecting brain activation. In arterial spin labeling (ASL) perfusion fMRI, fast acquisition is even more crucial because of the combined effects of the time needed to label the arterial water and the signal deterioration due to T_1 relaxation [1]. Fast acquisition comes at the expense of spatial resolution. While anatomical MRI images can be acquired at sub-millimeter level, the voxel sizes commonly used in fMRI are at least an order of magnitude higher [2]. This comparatively low spatial resolution of fMRI exacerbates the partial volume effects (PVE), defined as the mixing of the signals originating from different tissues present in a given voxel [3]. Mnimizing the confound of tissue-mixing in ASL imaging is essential for measuring changes in gray matter (GM) CBF due to aging and disease independently from concurrent anatomical changes such as those due to atrophy and lesions [4].

We have developed a tissue specific, ts-ASL, method that corrects for PVE by producing 'flow density' images that are independent of tissue mass. In other words, the 'flow density' value at a given voxel for a given tissue represents the amount of blood flow the voxel would have if it were comprised entirely of that tissue [3]. For example, when using ts-ASL, a voxel with 50% gray matter (GM) and 50% cerebrospinal fluid (CSF) would, theoretically, yield the same flow density value as a voxel that is 100% GM [3].

In a recent longitudinal study on healthy young subjects, we showed that the inter-subject variability of CBF using ts-ASL was about 40% lower than that of conventional ASL [5]. We speculated that the superior performance of ts-ASL was due to the fact that its signal is less affected by the anatomical variability across subjects. However, repeat acquisition on the same subject (data unpublished) indicated that the noise in ts-ASL images was lower even in the absence of anatomical variability. Because it is difficult to separate the sources of noise in experimental data, we decided to use simulated data so that we could control for the noise in functional images and anatomical variability in structural images independently. To this end, the SNR of the ts-ASL method was compared to that of the conventional ASL for increasing levels of noise and atrophy.

II. Theory

A. Conventional ASL

In all ASL methods, the proton spins of the arterial water are labeled prior to reaching the imaged volume by either saturation or inversion [6]. Once water is labeled, and after a time delay that allows for it to exchange with the tissue, a 'labeled' image, M_L, is acquired; the blood water protons in M_L are in a different magnetization state from those of the static brain tissue [1]. In addition to M_L, a 'control' image, M_C, is also acquired where the magnetization of the arterial water has not been altered, and, therefore, both the static tissue and the blood water protons are in the same magnetic state at the time of acquisition [1]. The difference between M_C and M_L cancels out the signal from the static tissue leaving only the signal from the labeled arterial spins.

The ASL signal is expressed as a ratio between the difference (M_C – M_L) image and the equilibrium magnetization, M_O, which for this study was taken as the average of M_C over the whole brain. [6]:

[1]Yujie Qiu and [*]Iris Asllani are with the Department of Biomedical Engineering, Rochester Institute of Technology, NY, USA (corresponding author, e-mail: icabme@rit.edu).

[2]Ajna Borogovac is with HAProxy Technologies Inc, USA.

[3]Andrew Laine is with the Department of Biomedical Engineering, Columbia University, NY, USA.

[4]Joy Hirsch is with the Department of Psychiatry and Neurobiology, Yale University, CT, USA.

978-1-4244-7929-0/14/$26.00 ©2014 IEEE

$$\text{ASL}_{\text{signal}} = \frac{(M_C - M_L)}{M_O} = \frac{\Delta M}{M_O} \quad (1)$$

A CBF image is computed in absolute physiological units of flow as:

$$f_{tissue} = (\Delta M / M_O) \cdot F_{tissue} \quad (2)$$

where F_{tissue} is a scaling factor that takes into account both physiological and MR parameters, such as partition coefficient and relaxation rates, for a given tissue [7].

B. Tissue-specific, ts-ASL

As mentioned above, given the relatively low spatial resolution of ASL, the ($\Delta M/M_O$) term contains contributions from all three brain tissues: gray matter (GM), white matter (WM), and CSF. Ideally, we want to be able to separate these contributions and compute CBF independently for GM and WM as:

$$f^p_{GM} = P_{GM} \cdot (\frac{\delta m_{GM}}{m_{GM}}) \cdot F_{GM} \quad (3)$$

$$f^p_{WM} = P_{WM} \cdot (\frac{\delta m_{WM}}{m_{WM}}) \cdot F_{WM} \quad (4)$$

and compute the net CBF as a sum of these partial contributions:

$$f_{NET} = f^p_{GM} + f^p_{WM} \quad (5)$$

To achieve this, we would need to estimate all five parameters – m_{GM}, m_{WM}, m_{CSF}, δm_{GM}, δm_{WM} – separately and for each voxel. As it stands, this is not possible because we have only 2 equations to estimate 5 parameters. However, by assuming that in a relatively small region surrounding each voxel these parameters remain constant, we can now bring more equations to bear by using linear regression to model M_C and ΔM as weighted sums of pure tissue contributions:

$$M_C(r_i) = P_j(r_i) \cdot m_j(r_i) \quad (6)$$

$$\Delta M(r_i) = P_j(r_i) \cdot \delta m(r_i) \quad (7)$$

where r_i is the position of each voxel, $P_j(r_i)$ is a row vector of the tissue type fraction at r_i, and $m_j(r_i)$ and $\delta m(r_i)$, which we seek to estimate, are column vectors of the equilibrium (M_C) and difference ($M_C - M_L$) intensities of the j^{th} tissue type at r_i, respectively. (See [3] for details.)

III. Methods

A. Image Acquisition

A high-resolution, magnetization prepared rapid gradient echo (MPRAGE) image was acquired on a healthy young subject on a 3T scanner (Philips Achieva), with the following parameters: TR/TE = 6.7 ms/3.1 ms, TI = 0.8 s, flip angle = 8°, spatial resolution = 0.9 x 0.9 x 0.9 mm^3, 180 slices. This image was used to simulate brain atrophy by varying the GM content of each voxel as described below.

To get a sense of the overall noise in the functional images, we looked at the spatial and temporal variation of the EPI signal from a longitudinal study [5].

B. Simulations of EPI, baseline CBF, and ΔCBF

Control and labeled EPI images were simulated as follows:

1) Voxelwise GM, WM, and CSF contents (in %) were obtained as posterior probability maps, P_{GM}, P_{WM}, P_{CSF}, from the tissue-segmentation of the MPRAGE using SPM8 unified segmentation algorithm [8].

2) The tissue content images were down-sampled to a typical EPI spatial resolution of 3.5 x 3.5 x 8 mm^3.

3) The control SE EPI ASL image (M_C) was modeled as:

$$M_C = (P_{GM} \cdot m_{GM}) + (P_{WM} \cdot m_{WM}) + (P_{CSF} \cdot m_{CSF}) \quad (8)$$

with tissue magnetization ratios assumed as: $m_{GM} = m_{WM} = m_{CSF}$ = 1.2/1/1.7 [3].

4) The labeled ASL image (M_L) was modeled as:

$$M_L = (P_{GM} \cdot (m_{GM} - \delta_{GM})) + (P_{WM} \cdot (m_{WM} - \delta_{WM})) + (P_{CSF} \cdot m_{CSF}) \quad (9)$$

where δ_{GM} and δ_{WM} represent the ($M_C - M_L$) difference images for GM and WM respectively. The values for δ_{GM} and δ_{WM} were back calculated using the 2-compartment formula [9] with the assumption that GM CBF = 80 mL/100g·min and WM CBF = 30 mL/100g·min, as per [4].

For all analysis, GM was defined by the voxels with GM content > 50%.

5) Matlab code was written to simulate ΔCBF ROI centered at a specified ROI by modifying the simulated SE EPI labeled image to reflect a 20% change in GM CBF (from a baseline of 80 mL/100g·min). Because of its role in aging and dementia and also because of its size, shape, and location in the brain, we selected the hippocampus as the ROI of choice. The hippocampal ROI, from pickatlas [10], was co-registered to the ASL imaging space and down-sampled to match the resolution of the EPIs. Although we show only results from the hippocampus, other ROIs with varying shape, size, and location were also investigated.

C. Image Processing and CBF Computation

CBF images were obtained using ts-ASL and the conventional method as described below:

Conventional ASL Method: ASL difference images were computed as ($M_C - M_L$) obtained above and were converted to CBF images using equations (1) - (2).

Ts-ASL Method: The algorithm that corrects for PVE was run on control and δ images as per equations (3) - (7) and as described in detail in our previous work [3].

D. Simulation of Noise

Uncorrelated zero mean Gaussian noise was simulated and introduced to the control and labeled images, independently, to account for a voxelwise standard deviation

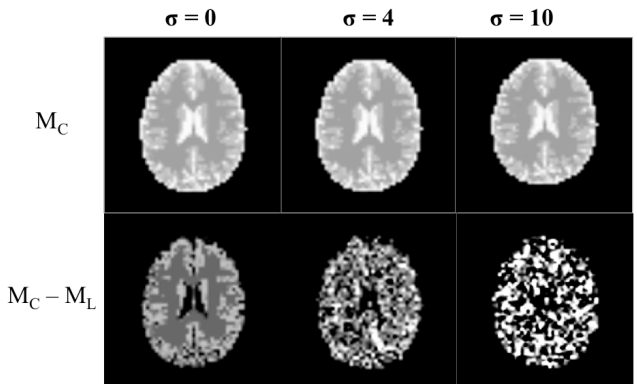

Fig.1A: Simulated control EPI images (M_C) and difference control-label ($M_C - M_L$) images for two different levels of noise, σ=4 and σ=10 and for the idealized situation of no noise, (σ=0).

(σ) of 4 and 10. We based these numbers on the intra-subject variance measurement of the ASL EPI images from our previous work [11].

E. *Simulation of Atrophy*

Atrophy was defined as a decrease (by a given percent) in GM tissue content. At each voxel, the GM content (obtained from the segmentation of the MPRAGE image) was decreased in the 0% - 25% range, step of 5%. Through this process, we simulated 6 GM (P_{GM}) posterior probability images; P_{WM} was not altered, P_{CSF} was increased correspondingly to keep the sum of probabilities to 1.

IV. Results

A. *Effect of Gaussian Noise on Estimating Baseline CBF: Comparison of ts-ASL with Conventional ASL fMRI.*

To give a sense of the images that were used to compute CBF for both ASL methods, control (M_C) EPIs and control-label (M_C–M_L) difference images are shown in Fig.1A; the corresponding GM CBF images are shown in Fig.1B. For all noise levels, the ts-ASL images more closely matched the simulated GM CBF (Fig.1B). Even in the idealized situation of zero noise, the conventional method was able to extract only about 80 % of the GM CBF signal, whereas ts-ASL, which is independent of voxels' tissue content, extracted 100% of it.

Quantitative results are shown in Fig.2. Note that even for σ=4 (expected to be comparable with actual noise in EPI imaging of healthy young volunteers at 3T [11]), the conventional method missed 80% of the CBF signal. In contrast, the effect of noise was lower for ts-ASL, which missed ~46% of the 'true' signal.

B. *Effect of Brain Atrophy on Estimating the CBF: Comparison of Conventional with ts-ASL fMRI.*

In the section above, the noise was introduced and varied only in the EPI (functional) images whereas the structural information was kept constant. In this section, we simulated brain atrophy by changing the GM content from 0% to 25% (step of 5%). The results for both ts- and conventional ASL are summarized in Fig.3A. As expected from theoretical

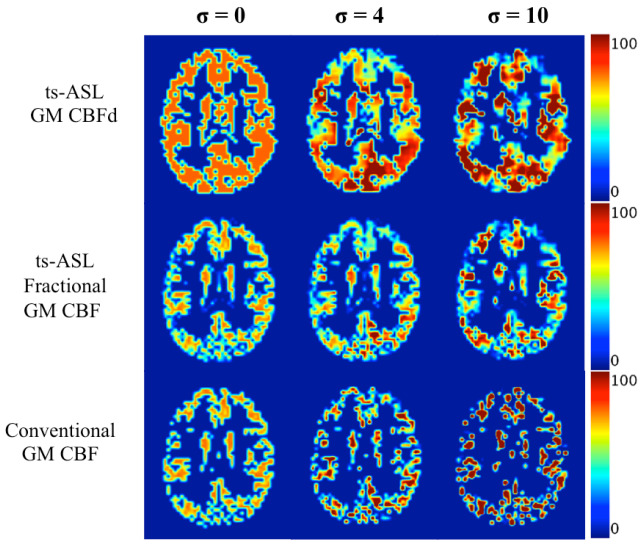

Fig.1B: 1st and 2nd rows: GM CBFd ('flow density') images and fractional GM CBF images obtained with ts-ASL. 3rd row: GM CBF images obtained with conventional ASL. Each column represents a different level of noise, starting with zero noise (σ=0).

considerations, because the ts-ASL method extracts CBF per tissue volume, it is largely independent of atrophy (Fig.3A, orange). In contrast, the error in estimating CBF using the conventional method increased with increasing atrophy (Fig.3A, blue). To get a visual sense of the effect of PVE on the GM CBF measurement, images are shown in Fig.3B.

C. *Combined Effects of Noise and Atrophy on the SNR of the Conventional and ts-ASL for Detecting Changes in CBF.*

The ability to detect changes in CBF is crucial for any fMRI method as these changes are expected to reflect changes in neural activity, which can be fast and short-term (brain activation) or gradual and long-term (aging and disease). In aging and disease, functional changes can occur concurrently with structural changes such as those associated with atrophy and/or lesions. Here, we tested the sensitivity of both methods for detecting changes in CBF (ΔCBF) in the presence of increasing levels of atrophy. We selected the hippocampus because of its relevance in studies of aging and dementia and also because of its shape and location in the brain (see Methods). As shown in Fig.4, even in the idealized situation of no noise, ts-ASL had higher sensitivity for detecting ΔCBF than conventional ASL. For combined

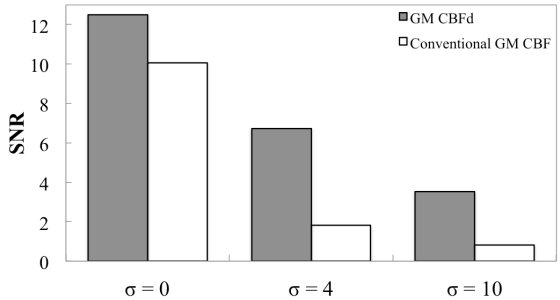

Fig.2: SNR obtained with ts-ASL GM CBFd (gray), and conventional ASL (white) at noise levels σ=4, σ=10 as well as in the absence of noise, σ=0, respectively. Note that ts-ASL had higher SNR than the conventional method for all the noise levels.

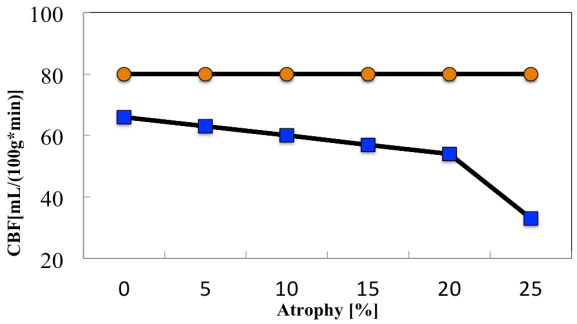

Fig.3A: Effect of brain atrophy on the accuracy of GM CBF measurement using ts-ASL GM CBFd (orange dots) and conventional ASL (blue squares).

15% atrophy and Gaussian noise with σ=4, ts-ASL retrieved 90% of ΔCBF, whereas conventional retrieved 73% of it.

V. Discussion and Conclusions

We compared two ASL fMRI approaches for obtaining CBF images: the conventional method and the tissue-specific method, which corrects for PVE by estimating the CBF for each tissue independently [3]. The comparison was done using simulated data containing various degrees of noise, mimicking a range of CBF variability observed in ASL studies conducted by our group and others ([4], [9], [11], [14]). For all scenarios, ts-ASL was superior to the conventional method by more closely matching the simulated CBF. Furthermore, the results showed that ts-ASL was minimally affected by anatomical variability and therefore can be used to detect changes in CBF (i.e., functional changed) independently from structural changes. One of the drawbacks of the ts-ASL method, however, is the inherent smoothing of the data (as can be seen in Fig.4), which can restrict its sensitivity in detecting small, localized changes in CBF.

Because aging and disease can concurrently affect both brain structure and function, developing a method that can measure these effects separately is essential for understanding the mechanisms underlying these effects and for development of biomarkers.

Acknowledgment

We thank Matthias J.P. van Osch for his thorough and rigorous critique of this work, which made it stand on stronger grounds and fine-tuned our strategy for future experiments.

References

[1] D. C. Alsop and J. A. Detre, "Reduced transit-time sensitivity in noninvasive magnetic resonance imaging of human cerebral blood flow," J Cereb Blood Flow Metab, vol. 16, 1996.

[2] A. Borogovac and I. Asllani, "Arterial spin labeling (asl) fmri: advantages, theoretical constrains, and experimental challenges in neurosciences," Int J Biomed Imaging, vol. 2012, 2012.

[3] I. Asllani, A. Borogovac, and T. R. Brown, "Regression algorithm correcting for partial volume effects in arterial spin labeling mri," Magn Reson Med, vol. 60, 2008.

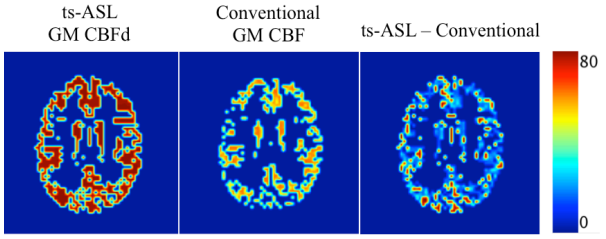

Fig.3B: GM CBF images obtained with ts-ASL CBFd (left) and conventional ASL (middle) for 20% gray matter atrophy in the absence of noise. Note that while the ts-ASL GM CBFd image is virtually homogenous, the conventional ASL GM CBF is dependent on tissue content, which can be quite heterogenous in the cortical boundaries.

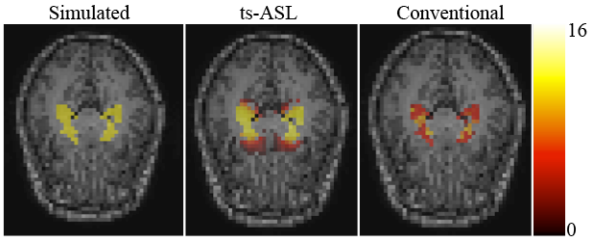

Fig.4: Concurrent structural (15% atrophy) and functional (20% GM CBF decrease) were simualted in the hippocampal-ROI resulting in a net ΔCBF = 16 mL/100g·min shown by the yellow ROI overlayed on the structural image (left). The CBF images extracted with ts-ASL (middle) and conventional ASL (right) show that ts-ASL more closely matched the functional change in CBF.

[4] I. Asllani, C. Habeck, A. Borogovac, T. R. Brown, A. M. Brickman, and Y. Stern, "Separating function from structure in perfusion imaging of the aging brain," Hum Brain Mapp, vol. 30, 2009.

[5] A. Borogovac, C. Habeck, S. A. Small, and I. Asllani, "Mapping brain function using a 30-day interval between baseline and activation: a novel arterial spin labeling fmri approach," J Cereb Blood Flow Metab, vol. 30, 2010.

[6] D. S. Williams, J. A. Detre, J. S. Leigh, and A. P. Koretsky, "Magnetic resonance imaging of perfusion using spin inversion of arterial water," Proc Natl Acad Sci U S A, vol. 89/1, 1992.

[7] J. Wang, D. C. Alsop, L. Li, J. Listerud, J. B. Gonzalez-At, M. D. Schnall, and J. A. Detre, "Comparison of quantitative perfusion imaging using arterial spin labeling at 1.5 and 4.0 tesla," Magn Reson Med, vol. 48, 2002.

[8] J. Ashburner and K. J. Friston, "Voxel-based morphometry–the methods," Neuroimage, vol. 11, 2000.

[9] L. M. Parkes, "Quantification of cerebral perfusion using arterial spin labeling: two-compartment models," J Magn Res Imag., vol. 22, 2005.

[10] J. A. Maldjian, P. J. Laurienti, R. A. Kraft, and J. H. Burdette, "An automated method for neuroanatomic atlas-based interrogation of fmri data sets," Neuroimage, vol. 19, 2003.

[11] I. Asllani, A. Borogovac, C. Wright, R. Sacco, T. R. Brown, and E. Zarahn, "An investigation of statistical power for continuous arterial spin labeling imaging at 1.5 t," Neuroimage, vol. 39, 2008.

[12] I. Asllani, C. Habeck, N. Scarmeas, A. Borogovac, T. R. Brown, and Y. Stern, "Multivariate and univariate analysis of continuous arterial spin labeling perfusion MRI in Alzheimer's disease," J Cereb Blood Flow Metab, vol. 28, pp. 725-36, Apr 2008.

[13] X. Golay, J. Hendrikse, and T. C. Lim, "Perfusion imaging using arterial spin labeling," Top Magn Reson Imaging, vol. 15, pp. 10–27, 2004.

[14] S. Gevers, M. J. van Osch, R. P. Bokkers, D. A. Kies, W. M. Teeuwisse, C. B. Majoie, et al., "Intra- and multicenter reproducibility of pulsed, continuous and pseudo-continuous arterial spin labeling methods for measuring cerebral perfusion," J Cereb Blood Flow Metab, vol. 31, pp. 1706-15, Aug 2011